Geomagnetic paleointensity between 1300 and 1750 AD derived from a bread oven floor sequence in Lubeck, Germany

Elisabeth Schnepp, Philippe Lanos, Annick Chauvin

Geochemistry Geophysics Geosystems G3
AN ELECTRONIC JOURNAL OF THE EARTH SCIENCES
Published by AGU and the Geochemical Society

Article
Volume 10, Number 8
5 August 2009
Q08003, doi:10.1029/2009GC002470
ISSN: 1525-2027

Geomagnetic paleointensity between 1300 and 1750 A.D. derived from a bread oven floor sequence in Lübeck, Germany

Elisabeth Schnepp
Paleomagnetic Laboratory Gams, Chair of Geophysics, University of Leoben, Gams 45, A-8130 Frohnleiten, Austria (elisabeth.schnepp@unileoben.ac.at)

Philippe Lanos
Laboratoire d'Archéomagnétisme, UMR 5060, Centre de Recherches en Physique Appliquée à l'Archéologie, Université Bordeaux 3, CNRS, F-35042 Rennes CEDEX, France

Also at Géosciences-Rennes, UMR 6118, Université de Rennes 1, CNRS, Campus de Beaulieu, CS 74205, F-35042 Rennes CEDEX, France

Annick Chauvin
Géosciences-Rennes, UMR 6118, Université de Rennes 1, CNRS, Campus de Beaulieu, CS 74205, F-35042 Rennes CEDEX, France

[1] Geomagnetic paleointensities have been determined from a single archaeological site in Lübeck, Germany, where a sequence of 25 bread oven floors has been preserved in a bakery from medieval times until today. Age dating confines the time interval from about 1300 A.D. to about 1750 A.D. Paleomagnetic directions have been published from each oven floor and are updated here. The specimens have very stable directions and no or only weak secondary components. The oven floor material was characterized rock magnetically using Thellier viscosity indices, median destructive field values, Curie point determinations, and hysteresis measurements. Magnetic carriers are mixtures of SD, PSD, and minor MD magnetite and/or maghemite together with small amounts of hematite. Paleointensity was measured from selected specimens with the double-heating Thellier method including pTRM checks and determination of TRM anisotropy tensors. Corrections for anisotropy as well as for cooling rate turned out to be unnecessary. Ninety-two percent of the Thellier experiments passed the assigned acceptance criteria and provided four to six reliable paleointensity estimates per oven floor. Mean paleointensity values derived from 22 oven floors show maxima in the 15th and early 17th centuries A.D., followed by a decrease of paleointensity of about 20% until 1750 A.D. Together with the directions the record represents about 450 years of full vector secular variation. The results compare well with historical models of the Earth's magnetic field as well as with a selected high-quality paleointensity data set for western and central Europe.

Components: 9239 words, 10 figures, 4 tables.

Keywords: paleointensity; secular variation; archaeomagnetism; Germany; Bayesian modeling.

Index Terms: 1521 Geomagnetism and Paleomagnetism: Paleointensity; 1503 Geomagnetism and Paleomagnetism: Archeomagnetism; 1522 Geomagnetism and Paleomagnetism: Paleomagnetic secular variation.

Received 3 March 2009; **Revised** 6 May 2009; **Accepted** 15 June 2009; **Published** 5 August 2009.

Schnepp, E., P. Lanos, and A. Chauvin (2009), Geomagnetic paleointensity between 1300 and 1750 A.D. derived from a bread oven floor sequence in Lübeck, Germany, *Geochem. Geophys. Geosyst.*, *10*, Q08003, doi:10.1029/2009GC002470.

1. Introduction

[2] Time series of the three elements (inclination, declination, intensity) of the Earth's magnetic field (EMF) are needed for global modeling of the field [*Jackson et al.*, 2000; *Korte and Constable*, 2003, 2005] in order to obtain a better understanding of the processes in the geodynamo situated within the Earth's outer liquid core. While polarity transitions are only known from paleomagnetic records, the secular variation, which is a slow change of direction and intensity, is determined from direct observations covering the past 400 years. These historical measurements of continuous recording of the EMF's direction started in the 16th century [e.g., *Alexandrescu et al.*, 1997] first with observation of declination. Inclination records started together with relative intensity measurements at the end of the 17th century and no absolute intensities were recorded before the 1830s [*Jonkers et al.*, 2003].

[3] Our knowledge on the EMF's history for earlier times comes from paleomagnetic measurements on well dated rocks or archaeological artifacts. A recent global compilation of archaeomagnetic and paleomagnetic data [*Korte et al.*, 2005] was used to derive a global field model for the past 7000 years [*Korte and Constable*, 2005]. Although such a modeling of the EMF is possible using only directional data if an assumption about the axial dipole strength is made, intensity data are crucial for obtaining models without a priori assumptions or testing such calibration assumptions. For the paleomagnetic as well as for archaeomagnetic data sets the portion of intensity data is much smaller than for direction. Apart from this many intensity data were obtained from displaced material, especially potsherds, and so no corresponding directions are available. For western Europe, *Chauvin et al.* [2000] compiled all available archaeointensity data of the past 2000 years and classified them by a weighting factor based on number and type of the samples as well as on the technique used for paleointensity determination. Their conclusion was that most of the existing data may not be reliable. *Gallet et al.* [2005] and *Genevey and Gallet* [2002] presented high-precision paleointensity data from French pottery and found large variations during the past 2000 years, but only in a few cases these temporal variations are confirmed by multiple sets of archaeological material of the same age. Such a test was carried out by *Gómez-Paccard et al.* [2006] on almost contemporaneous kilns from Spain. Although corrections of anisotropy and cooling rate have been carried out large differences have been observed between these contemporaneous structures. Global compilations of paleointensity data for the past 10 millennia [*Genevey et al.*, 2008; *Korhonen et al.*, 2008] comprising about 3600 data, mainly obtained from archaeological artifacts, also show a large dispersion of the intensities. Application of simple and rather weak selection criteria, like demanding application of a reliable paleointensity method, at least three paleointensity experiment results per structure, a standard deviation of less than 15% of the estimated value, and correction of anisotropy for strongly anisotropic materials like potsherds retains only about 18% of the data, while application of severe criteria diminishes the set to only 110 values [*Genevey et al.*, 2008]. Accordingly new paleointensity data fulfilling such strict criteria are still needed.

[4] This paper presents a full vector record of about 450 years of secular variation from a single archaeological site in Lübeck, Germany, where a sequence of 25 bread oven floors were preserved in a bakery from medieval times until today. The directional record was already published [*Schnepp et al.*, 2003] and is supplied with paleointensities here.

2. Paleomagnetic Directions of the Lübeck Oven Floor Sequence and Age Dating

[5] Archaeological excavations uncovered seven ovens in a baker's house in Lübeck, Germany [*Müller*, 1992], each built upon its predecessor. Four of the ovens had circular domes, each with several consecutive floors of baked loam inside. There are 25 oven floors still extant, adding up to a height of roughly 1.1 m. Since the fires to heat the oven burned on these floors, their smooth finish would have become rough, making the bread stick, so regularly new floors were added. Because the inner height of the oven was reduced by this, it

would become necessary to rebuild the dome regularly, too.

[6] For the paleomagnetic investigation at least six oriented hand samples per layer have been taken from the pile of 25 oven floors, but only less for the layers 11 and 13 which were very thin and unconsolidated. The sampling procedure, the preparation of the samples, the applied rock magnetic and paleomagnetic measurements and age dating have been described by *Schnepp et al.* [2003] and the results are summarized in the following.

[7] Paleomagnetic direction has been determined by alternating field and thermal demagnetization of 425 specimens. About 90% of the specimens show only weak secondary components, which were removed by 10 mT or 250°C. The median destructive temperature (MDT) was mostly between 300°C and 500°C. Accordingly, most specimens are characterized by a very stable single component thermoremanent magnetization (TRM) which is a prerequisite for successful paleointensity determination. Well defined characteristic remanent magnetization directions were obtained from principal component analysis (PCA). Mean directions have been calculated for 24 of the oven layers. They are characterized by small α_{95} confidence circles and reflect significant directional variations which provide a record of secular variation. The age model of the oven floor sequence is based on one ^{14}C date for layer 25 using the acceleration mass spectrometry technique, thermoluminescence (TL) dating of 11 oven floors, historical documents and comparison with historical magnetic records. The mean directions provide a secular variation curve for Lübeck covering the time interval from about 1300 to 1750 A.D.

3. Rock Magnetic Results and Suitability for Paleointensity Determination

[8] Rock magnetic results have been presented by *Schnepp et al.* [2003] and they are completed here. The rock magnetic characteristics are very similar for the specimens from all oven floor layers, but the concentration of the magnetic carriers varies between the layers and it also decreases with depth in each layer [cf. *Schnepp and Pucher*, 1998, Figure 2]. Almost all specimens have Koenigsberger ratios above 2 [cf. *Schnepp et al.*, 2003, Figure 6a] suggesting that the natural remanent magnetization (NRM) is a thermoremanent magnetization formed during heating and cooling of the bread ovens. Curie points lie between 570 to 620°C [cf. *Schnepp et al.*, 2003, Figure 5b]. The magnetic carriers are accordingly magnetite with a small amount of impurities, maghemized magnetite or stable maghemite. Regardless which carrier of magnetization dominates, the minerals are very stable during heating and almost reversible thermomagnetic curves were obtained [cf. *Schnepp et al.*, 2003, Figure 5b]. In many specimens also a small amount of hematite is present carrying less than 10% and in a few cases up to 20% of saturation isothermal remanent magnetization at 3 T [cf. *Schnepp et al.*, 2003, Figure 5a].

[9] During thermal demagnetization experiments susceptibility was measured after each heating step. Here moderate changes of susceptibility with temperature occurred: This was either a weak increase of about 5% at 200°C or 500°C or a decrease of up to 20% (in very few cases 30%) at 500 to 550°C, sometimes also a small increase followed by a decrease was observed. Furthermore, viscosity indices of 215 specimens were measured with the method of *Thellier and Thellier* [1944]. In most cases they were very low (less than 5%) and they never exceeded 16% [cf. *Schnepp et al.*, 2003, Figure 6b]. More than 200 alternating field demagnetizations confirmed very stable remanence directions. The median destructive field (MDF) values obtained from these AF demagnetizations are in most cases between 15 and 20 mT [cf. *Schnepp and Pucher*, 1998, Figure 6b]. Although some specimens gave lower MDFs, only two specimens undercut the value of 12.9 mT which was identified by *Carvallo et al.* [2006] as a threshold for successful Thellier experiments.

[10] In order to characterize the magnetic domain state measurements of apparent hysteresis loops and isothermal remanent magnetization (IRM) with acquisition and backfield curves have been carried out with a Princeton Micromag AGFM for one small piece (2 to 17 mg) from each layer. Furthermore IRM acquisition had already been studied for the cubic specimens (approximately 20 g [*Schnepp et al.*, 2003, Figure 5a]). While the remanent coercive force B_{cr} for the large cubic specimens lies in a narrow interval between 20 and 30 mT, the variation is much bigger for the small chips measured in the Micromag (Figure 1a). The chips show a bimodal distribution of B_{cr}, while the results from the big cubic samples fall into this gap. This gives evidence that the grain size distribution is not continuous but comprises two populations of magnetic grains in each specimen.

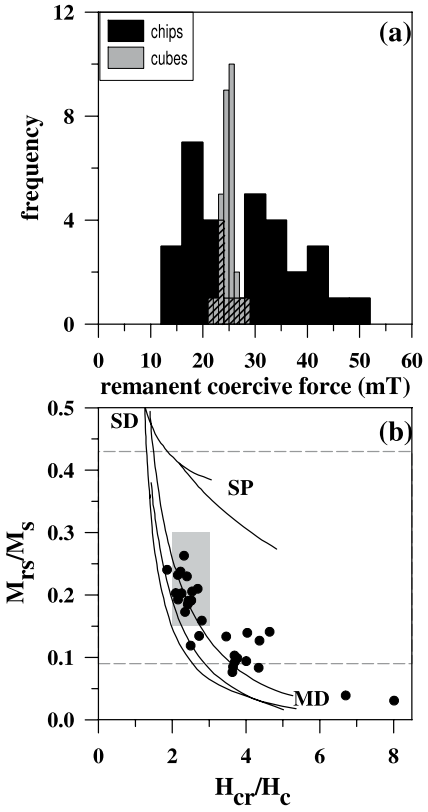

Figure 1. Hysteresis parameters of the Lübeck samples. (a) Histogram of the remanent coercive force obtained from isothermal remanent magnetization (IRM) acquisition of cubic specimens [see *Schnepp et al.*, 2003] (gray and hatched bars) and from small chips (black and hatched bars) measured in an alternating gradient force magnetometer. (b) Day diagram [*Day et al.*, 1977]: ratio of saturation magnetizations is plotted versus ratio of coercivities. The black lines were obtained by *Dunlop* [2002] for mixtures of SD and MD grains, and the gray area was identified as typical for pottery. Dashed lines indicate the range which *Hill et al.* [2007] found for pottery kilns.

[11] A large dispersion of the hysteresis data is observed as well, when the results of the hysteresis measurements are plotted in a Day diagram [*Day et al.*, 1977] (Figure 1b). The ratios of coercivities and magnetizations imply that the Lübeck samples are dominated by pseudo single domain (PSD) grains and that a minor fraction of larger grains is present, which can have also true multidomain (MD) size. Taking into account that the samples seem to contain two populations of magnetic grains the results in the Day plots can also be explained by mixtures of SD and MD grains. About half of the data points plot in the region which was identified by *Dunlop* [2002] as typical for pottery (gray bar). Most of the Lübeck hysteresis data show the same range in the Day diagram as data for pottery kilns published by *Hill et al.* [2007], which provided very good paleointensity results.

[12] Apart from nonideal behavior during the Thellier experiments, strong magnetic anisotropy and/or cooling rate dependence of the TRM acquisition could be further obstacles for the determination of reliable paleointensities. The B_{cr} values obtained for the Lübeck samples are much lower than those expected for elongated SD magnetite [e.g., *Schlinger et al.*, 1991], and according to *Schnepp et al.* [2003, Figure 5c] no elongated magnetic particles are present. Although the smoothing of the loam or clay during fabrication of the oven floor may have introduced some alignment of the clay particles a strong TRM anisotropy generally has not to be expected for baked clay [*Kovacheva et al.*, 2009]. Nevertheless the presence of TRM anisotropy was tested during the Thellier experiments and will be exemplified in section 4.

[13] For the oven type found in Lübeck the combustion and baking chamber are one and the same. The maximum temperature reached by such a bread oven floor is about 800°C, when the oven is heated up. Then the oven is rapidly cooled down to the operation temperature of about 290°C, because the burning wood and the ash are completely removed before inserting the bread. During baking the temperature is further decreasing to 210°C (R. Pucher and W. Brandes, personal communication, 1998). Accordingly, the cooling rate of the ovens is rather quick and in an order which can be reproduced on laboratory scale, but the exact cooling rate is not known. In summary the Lübeck

Figure 2. Examples of Thellier experiments with different quality factors: (a) highest, (b and c) moderate, (d and e) low, and (f) rejected. See text for details (see Figure 4 and Table S1 in the auxiliary material). Arai plot with natural remanent magnetization (NRM) plotted against the partial thermoremanent magnetization (TRM) gained at temperature steps indicated in °C. pTRM checks are shown by arrows. Specimen name and obtained paleointensity are given. Data points used for the regression line are shown as solid black circles, and rejected ones are shown as open black circles. The inset in the top right corner of each Arai plot is the orthogonal projection of directions obtained during the Thellier experiment. Y versus X component is plotted with solid symbols, while open symbols are vertical versus horizontal component.

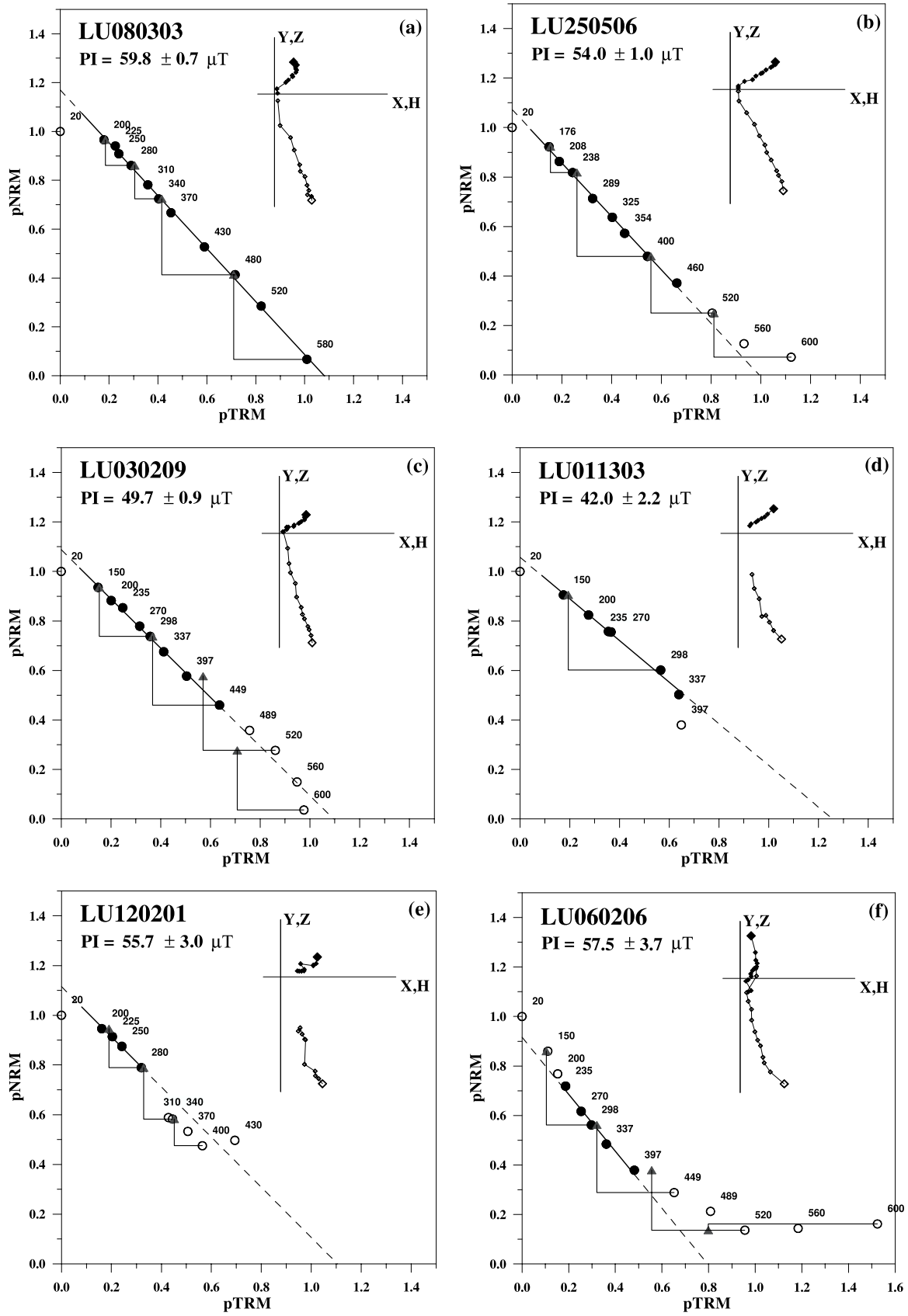
LU080303
PI = 59.8 ± 0.7 μT
(a)
LU250506
PI = 54.0 ± 1.0 μT
(b)
LU030209
PI = 49.7 ± 0.9 μT
(c)
LU011303
PI = 42.0 ± 2.2 μT
(d)
LU120201
PI = 55.7 ± 3.0 μT
(e)
LU060206
PI = 57.5 ± 3.7 μT
(f)
Y,Z
X,H
pNRM
pTRM

Figure 2

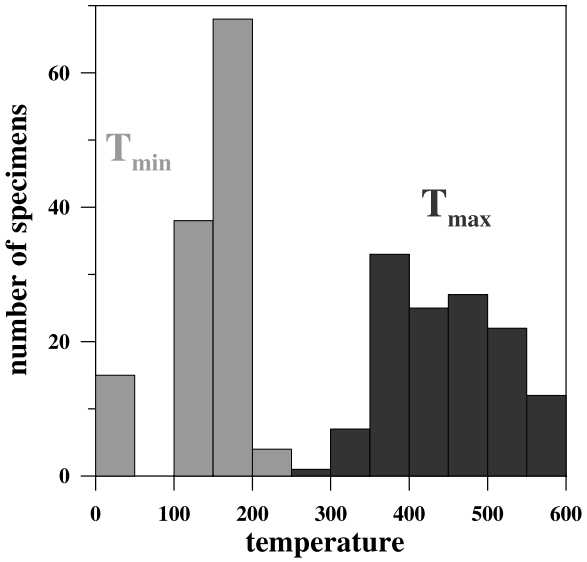

Figure 3. Maximum (dark gray) and minimum (light gray) temperature of the range from which paleointensity was obtained from the Thellier experiments.

oven floors seem to provide a material promising to be well suited for paleointensity determination.

4. Paleointensity Experiments

4.1. Thellier Experiments

[14] For 22 of the 25 oven floors a sufficient number of untreated specimens was available for the paleointensity study. 127 specimens from these oven floors have been subjected to Thellier experiments using the original method [*Thellier and Thellier*, 1959] with 12 or 13 heating steps between 150°C and 600°C in a field of 50.0 (in Montpellier and 55.2 in Rennes) μT. Four pTRM checks have been carried out. The specimens were measured in two laboratories with different equipments. 71 specimens were measured in Montpellier. Here the paleointensity oven provided a vacuum better than 10^{-2} mbar and laboratory field intensity was held with a precision of 0.1 μT. The cooling circle took about 8 h. Magnetization was measured with a CTF cryogenic magnetometer. 56 specimens were measured in Rennes using a MMTD60 thermal demagnetizer and a Minispin magnetometer. Here cooling of the specimens took about 30 min. After each temperature step bulk susceptibility was measured using a Bartington bridge. In both sets many specimens were very brittle and lost material after reaching 250°C. Therefore a correction for loss of mass was applied after each heating step [*Schnepp*, 2003]. Twenty-six specimens were destroyed before reaching the maximum temperature of 600 (580) °C.

[15] For most specimens a very weak secondary component was removed by the first temperature steps up to 250°C (see Figure 2) and these data points were rejected for evaluation of paleointensity and direction. After that, most Thellier experiments provided straight lines to the origin in the modified Zijderveld diagrams with maximum angular deviation (MAD) less than 2° and a linear segment in the Arai plots, with at least one positive pTRM check. If present, weak alteration or non-ideal behavior of the specimens started around 350°C leading to a concave-up or concave-down curvature of the line defined by the data points in the Arai plots and for these specimens also the pTRM checks indicate a change of pTRM capacity.

[16] Nevertheless, in all cases adjustment of a regression line was possible and (with one exception) at least five data points were available to calculate the slope with corresponding correlation coefficient and gap, fraction and quality factors of *Coe et al.* [1978] (Table S1 in the auxiliary material).[1] The temperature range from which paleointensity was calculated is indicated in Figure 3, while Figure 4 summarizes the correlation coefficients, numbers of data points, fraction factors, and quality factors. Acceptance limits are indicated by the gray boxes, namely results were accepted with a slope determined by more than five data points, a fraction factor above 20%, a quality factor above 5, and a correlation coefficient above 0.985. Only ten Thellier experiments with low-quality factors and/or fraction factors (open symbols) were judged to be unreliable. However, four Thellier experiments were accepted despite the very low fraction factors or correlation coefficients, because the specimens were broken at low temperatures and no alteration was seen.

[17] Six examples of Arai plots are shown in Figure 2 (main plots) and the detailed results are given in Table S1 of the auxiliary material, while the quality parameters of these Thellier experiments are highlighted in Figure 4. The first example (Figures 2a and 4) provided a very high quality factor. Here the data points are aligned almost perfectly on a straight line and there is no deviation of the pTRM checks. Nevertheless, NRM has been excluded from paleointensity evaluation because there is a small secondary overprint present (see

[1] Auxiliary materials are available at ftp://ftp.agu.org/apend/gc/2009gc002470.

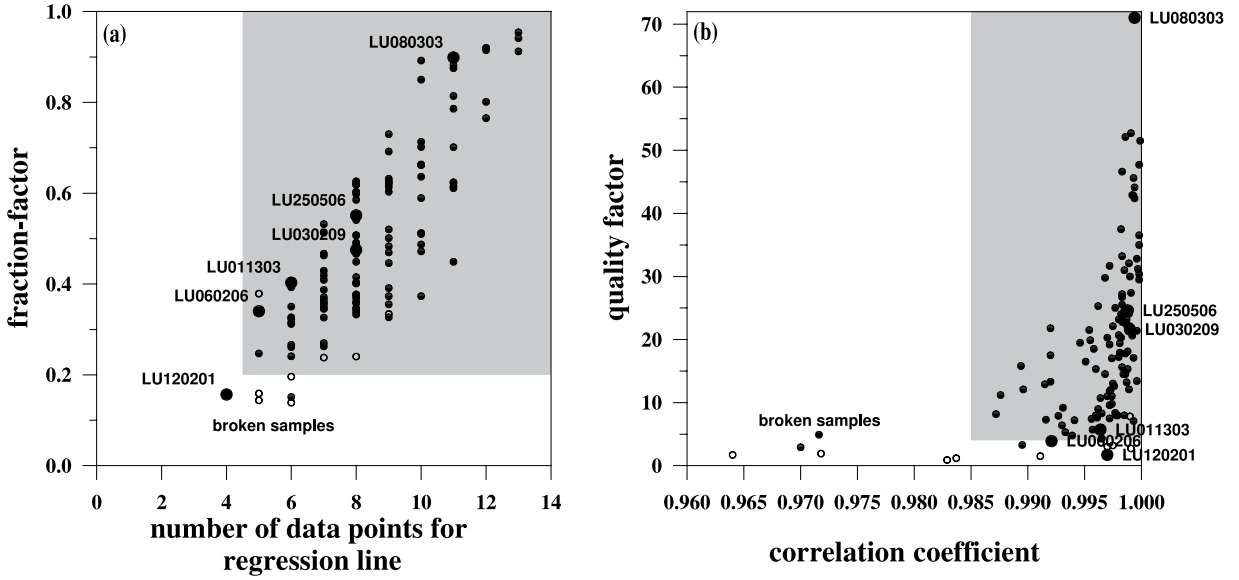

Figure 4. Quality of the Thellier experiments: (a) Fraction factor [*Coe et al.*, 1978] is plotted versus number of data points used for evaluation of the slope. (b) Coe quality factor is plotted versus correlation coefficient. Examples from Figure 2 are indicated by large dots and specimen name. Shaded areas give acceptation criteria (see text).

orthogonal projection in Figure 2a). Figures 2b and 2c are representative for most of the results obtained. After removal of a small secondary component, a straight line on the Arai plot arises in general between 160 and 460°C. Here the fraction of NRM used to evaluate paleointensity is around 60%. Although for specimen LU250506 (Figure 2b) no failure of the pTRM checks is observed above 400°C the data points start to form a concave down line. Hysteresis parameters of a sister specimen plot in the PSD range but it seems that at higher temperatures the MD grains present in the specimen disturb the Thellier experiment. On the contrary specimen LU030209 (Figure 2c) shows a considerable change in pTRM capacity above 450°C which is indicated by failure of the pTRM checks (more than 7.5% of NRM). Nevertheless up to this temperature a very well defined straight line is observed in the Arai plot as well as in the orthogonal projection of direction.

[18] Figures 2d and 2e are examples for relatively poorly defined lines in the Arai plots. Both specimens were very brittle and completely fell apart around 400°C. Despite this, well defined linear segments are obtained as indicated by high correlation coefficients (see Figure 4). LU120201 shows some disturbance in the directional behavior, because this specimen was broken at 310°C. After gluing some misalignment of the fragments occurred. This was seen in a parallel displacement of the straight lines in the Arai plot as well as in the orthogonal projection plots. Nevertheless the pTRM checks worked well and this paleointensity result was accepted despite the fact that it is based only on four data points. Finally, Figure 2f shows a rejected result which obviously shows a disturbed behavior during the Thellier experiment. Data points in the Arai plot form a concave line and this is also true for the five data points tentatively selected for a regression line. A strong change in TRM capacity is recorded by the pTRM checks (more than 7.5% of NRM). The directional lines in the orthogonal plot are distorted from origin. Such a behavior is typical for MD grains and hysteresis parameters of the sister specimen plot close to the MD range. In most cases paleointensity results were not rejected because of a disturbed Thellier experiment giving a curved line in the Arai plot or because of directional change introduced by the Thellier experiment. But in both cases tentatively evaluated paleointensity gave low fraction and or quality factors and this was criterion of rejection (see Figure 4).

4.2. TRM Anisotropy

[19] Because smoothing of the loam during construction of an oven aligns the mineral grains at least close to the surface, this fabric may result in anisotropy of the magnetic properties. If this anisotropy affects also the remanence carrying grains, it would be seen in the laboratory TRM depending on direction in the floor. If in the Thellier exper-

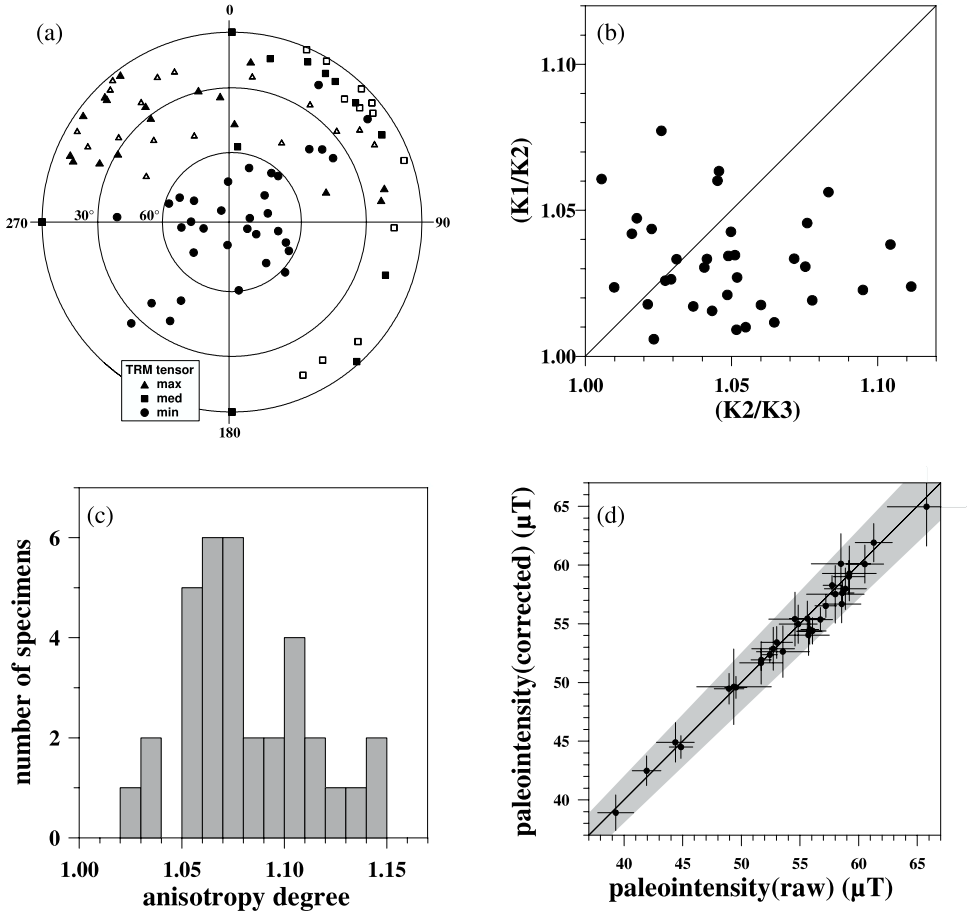

Figure 5. Results of the TRM anisotropy test (see text): (a) equal area projection of principal axes of the TRM ellipsoid (open symbols lie on the lower half-sphere), (b) Flinn plot with lineation (K1/K2) plotted versus foliation (K2/K3) of the TRM ellipsoid, (c) histogram of the anisotropy degree, and (d) TRM anisotropy corrected paleointensity plotted versus uncorrected result. Grey area is ±5% limit.

iment the laboratory field would not be applied parallel to the paleodirection, the observed paleointensity would be dependent on direction of the applied field. Strong anisotropy of the TRM tensor is well known for tiles, bricks and pottery [*Chauvin et al.*, 2000; *Genevey and Gallet*, 2002] but may be much weaker for the baked clay of an oven [*Hill et al.*, 2007].

[20] For the Lübeck ovens anisotropy of the TRM was tested in Rennes laboratory and evaluated for 35 specimens following the procedure used by *Chauvin et al.* [2000]. At 480°C, when between 20 and 50% of NRM was left additional heating steps were performed for most of the specimen, excluding those which were broken or had an irregular shape. After the usual heating in +Z and −Z direction and application of the pTRM check, further heatings in +X, −X, +Y, −Y and finally again in +Z direction were done. The last step was used to evaluate the change in TRM capacity and the derivation was in the range of −8% to +9% of the initial TRM in +Z. The change was in all cases less than ±15%, which was used by *Hill et al.* [2007] as rejection criterion. The anisotropy tensor was calculated as described by *Chauvin et al.* [2000] using the software RenArmag after application of the mass correction.

[21] Because the specimens taken for the Thellier experiments were cut perpendicularly to the original surface of the oven floors, the X−Y plane of the sample coordinate system lies parallel to it. Figure 5a shows a more or less vertical alignment of the short axis of the TRM ellipsoid. Accordingly for most of the specimens the short axis was aligned perpendicular to the direction of smoothing when the floor has been made. Most specimens show in the Flynn diagram oblate anisotropy (Figure 5b). Nevertheless, foliation as well as lineation is very weak compared to values reported for tiles and bricks [*Chauvin et al.*, 2000]. Also the

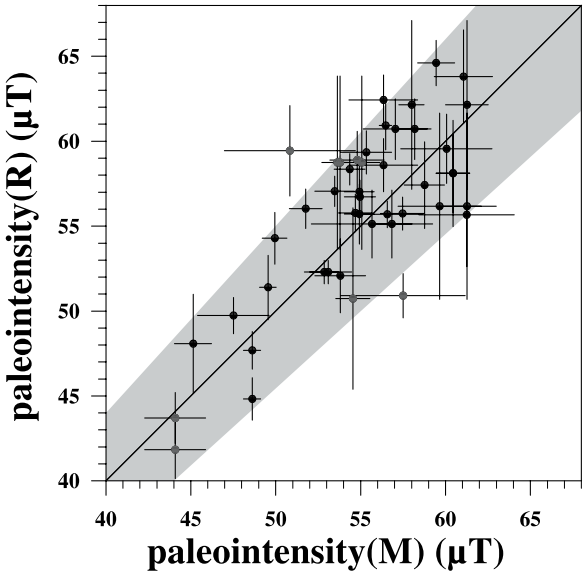

Figure 6. Paleointensity results obtained in Rennes plotted versus results of sister specimens measured in Montpellier with a much longer cooling cycle. Rejected results are indicated by gray dots. Grey area is ±10% limit.

degree of anisotropy is very low compared to pottery, for which *Genevey and Gallet* [2002] obtained values above 1.07 up to 1.98 (see Figure 5c). Furthermore with steep inclinations around 70° the archaeodirections are aligned close to the vertical axis which is more or less the Z axis of the specimens. During the Thellier experiments TRM was created in +/−Z direction and therefore close to the archaeodirection. Figure 5d compares the anisotropy corrected paleointensity values with those calculated without application of such a correction. The shaded area marks the 5% limit of change and Figure 5d demonstrates that for most specimens no significant change is observed. It was therefore decided that anisotropy correction is not necessary. TRM anisotropy correction also did not change significantly the ChRM directions.

4.3. Cooling Rate Dependence

[22] No classical experiment [e.g., *Chauvin et al.*, 2000; *Genevey and Gallet*, 2002] in order to evaluate cooling rate dependence has been performed. From operation of a modern bread oven build in the same style as the Lübeck ovens it is known that cooling is much quicker than for a pottery kiln. Before inserting the bread, the oven is cooled quickly down to its operation temperature (see above). Accordingly the cooling rate should have been somewhere between the quick cooling done in Rennes (30–40 min) and the slow cooling performed in Montpellier (approximately 8 h). Figure 6 compares the paleointensity values obtained from sister specimens, measured in Rennes and in Montpellier. The diagram shows an arbitrary distribution and differing cooling rates do not show any systematic influence on the paleointensity result. Except for two rejected paleointensity results all the data lie in the range of only 10% change. This is interpreted, that no significant dependence on cooling rate is seen in the time interval which has to be assumed for the original cooling rate. This does not exclude that a dependence on cooling rate may exist for slower cooling, as it would be expected for large PSD grains. Because cooling rate is not exactly known for these ovens, it was decided to omit any cooling rate correction.

5. Results

5.1. Paleodirection

[23] Apart from a paleointensity estimate each Thellier experiment provides a thermal demagnetization, which can be used to derive a characteristic remanent magnetization (ChRM) direction. Accordingly, the Thellier experiments gave new demagnetization series which were interpreted using the same principal component analysis procedure as described by *Schnepp et al.* [2003]. The majority of the successful Thellier experiments provided directions which can be classified as A(B) or C according to *Schnepp et al.* [2003], characterized by very small secondary magnetization components and MAD of less then 1.0° (class A and B) or up to 3.0° (class C). Only four specimens gave larger MAD up to 5.0°. 118 new paleodirections from 22 of the layers have been combined with the published results and new mean directions have been calculated with respect to hierarchical sampling levels of layer, hand sample and specimen [*Lanos et al.*, 2005].

[24] These updated directions are listed in Table 1 together with the assigned age model which takes comparison with historical directions into account [*Schnepp et al.*, 2003, Table 2]. The new directions are indistinguishable from the published results. Angular distances between old [*Schnepp et al.*, 2003] and new (combined) results exceed 0.5° only in three cases and they are always considerably lower than the α_{95} value. The Fisherian precision parameter was in most cases augmented and accordingly the α_{95} error cones were reduced. These new well defined and consistent directional

Table 1. Full Vector Paleomagnetic Results of the Lübeck Oven Floor Sequence[a]

Oven Floor	Assigned Age	Paleodirection						Paleointensity			
		N	D (deg)	I (deg)	r	k	α_{95}	n	F (μT)	σ_F (μT)	$\sigma_{Frel.}$ (%)
01	A.D. 1580–1750	14	343.6	73.7	13.981	686.8	1.5	5/7	44.1	3.3	7.5
02	A.D. 1580–1750	9	356.1	73.9	8.996	1803.2	1.2	5/6	46.6	1.3	2.9
03	A.D. 1580–1750	8	352.9	76.0	7.997	1980.8	1.2	5/5	50.6	1.9	3.8
04	A.D. 1580–1750	9	355.4	76.8	8.995	1502.0	1.3	6/6	47.4	2.2	4.6
05	A.D. 1580–1750	8	354.0	76.0	7.990	732.4	2.0	5/5	50.7	2.7	5.3
06	A.D. 1580–1750	7	359.0	74.9	6.995	1308.9	1.7	5/6	52.2	1.0	1.9
07	A.D. 1580–1750	9	357.5	76.5	8.994	1302.8	1.4	6/6	49.8	1.6	3.2
08	A.D. 1580–1750	9	13.2	72.4	8.979	380.8	2.6	6/6	58.9	1.9	3.3
09	A.D. 1580–1750	6	13.4	71.5	5.987	372.8	3.5	6/6	59.7	2.9	4.8
10	A.D. 1580–1750	8	15.9	70.5	7.978	323.0	3.1	5/5	55.8	1.8	3.3
11	A.D. 1517–1750	1	8.4	70.1	–	–	–	–	–	–	–
12	A.D. 1517–1709	7	15.1	69.9	6.991	695.2	2.3	5/5	58.8	3.0	5.2
13	A.D. 1502–1709	4	12.8	71.1	3.998	1498.5	2.4	–	–	–	–
14	A.D. 1502–1654	9	14.4	69.4	8.987	618.5	2.1	3/5	54.2	1.0	1.8
15	A.D. 1449–1654	9	14.7	68.2	8.986	585.6	2.1	6/6	55.0	2.2	4.1
16	A.D. 1449–1608	8	8.6	69.2	7.968	217.8	3.8	5/6	53.4	1.9	3.5
17	A.D. 1448–1608	8	5.0	68.1	7.969	224.6	3.7	6/7	58.5	3.9	6.6
18	A.D. 1448–1608	8	11.6	66.9	7.993	1009.3	1.7	5/5	58.2	1.7	2.9
19	A.D. 1428–1549	9	7.2	66.5	8.989	757.4	1.9	6/6	59.7	2.0	3.4
20	A.D. 1301–1549	10	4.3	65.2	9.973	335.3	2.6	6/6	60.4	2.9	4.9
21	A.D. 1301–1549	8	9.5	63.1	7.987	543.7	2.4	4/6	58.7	1.4	2.4
22	A.D. 1301–1500	8	3.4	64.5	7.957	162.5	4.4	–	–	–	–
23	A.D. 1301–1500	9	4.7	64.3	8.992	992.1	1.6	6/6	57.3	1.9	3.4
24	A.D. 1283–1500	8	9.7	63.5	7.985	466.3	2.6	6/6	56.0	1.0	1.8
25	A.D. 1283–1378	8	15.2	65.4	7.953	147.4	4.6	5/5	53.8	0.7	1.2

[a] Location is 53.867°N, 10.813°E. The oven floor number and the assigned age correspond to *Schnepp et al.* [2003], and paleodirection is hierarchical mean characteristic remanent magnetization direction (ChRM), obtained from alternating field, thermal demagnetization, and Thellier experiments. Paleointensity was obtained from Thellier experiments (see Table S1 in the auxiliary material). N, number of samples; D, mean declination; I, mean inclination of ChRM; r, vector sum; k, precision parameter; α_{95}, radius of 95% confidence limit of the Fisher statistics; n, number of Thellier experiments (accepted/performed); F, paleointensity; σ_F, standard deviation; $\sigma_{Frel.}$, relative error.

results obtained from the Thellier experiments underline that the paleointensity experiments rarely have been disturbed by MD grains, because the pTRM tails would have changed the directions [*Yu and Dunlop*, 2003].

5.2. Paleointensity

[25] Figure 7 shows a synthesis of 117 reliable paleointensity estimates (dots) of the Lübeck oven floors and the 10 rejected results (circles). The paleointensity values within floor layers show a very good agreement and significant changes between the oven floors are seen (see also Table S1 in the auxiliary material). For each oven floor the unweighted average paleointensity (thick line) is based on three to six results (Table 1). The mean is plotted together with the standard deviation (gray boxes) versus the floor number. The relative errors are very low and these values range from 1.2 to 7.5%, accordingly the paleointensity estimates are very precise. Paleointensities vary between 60 and 44 μT, which is close to the present value of 49 μT. Already the 22 mean results show a clear variation in paleointensity during the use of the bread ovens, which is interpreted as secular variation.

5.3. Bayesian Smoothing

[26] In order to obtain a smooth curve of geomagnetic secular variation for Lübeck we implemented hierarchical Bayesian modeling and fitted spherical spline functions based on a roughness penalty to the data. As there are full vector data available which vary with time three possibilities of fitting could be tested: (1) univariate distributions for declination, inclination, and intensity (and time); (2) a bivariate distribution for direction [*Schnepp et al.*, 2003] combined with a univariate distribution for intensity (and time); and (3) a full vector distribution (and time). The experimental errors of dating are taken into account by the hierarchy modeling and they were associated with stratigraphic observation of the layers, which provides a priori relative chronological information. The Bayesian model used here, allows all these observations to be linked together. Since the model takes account of all the known errors [*Lanos et al.*, 2005]

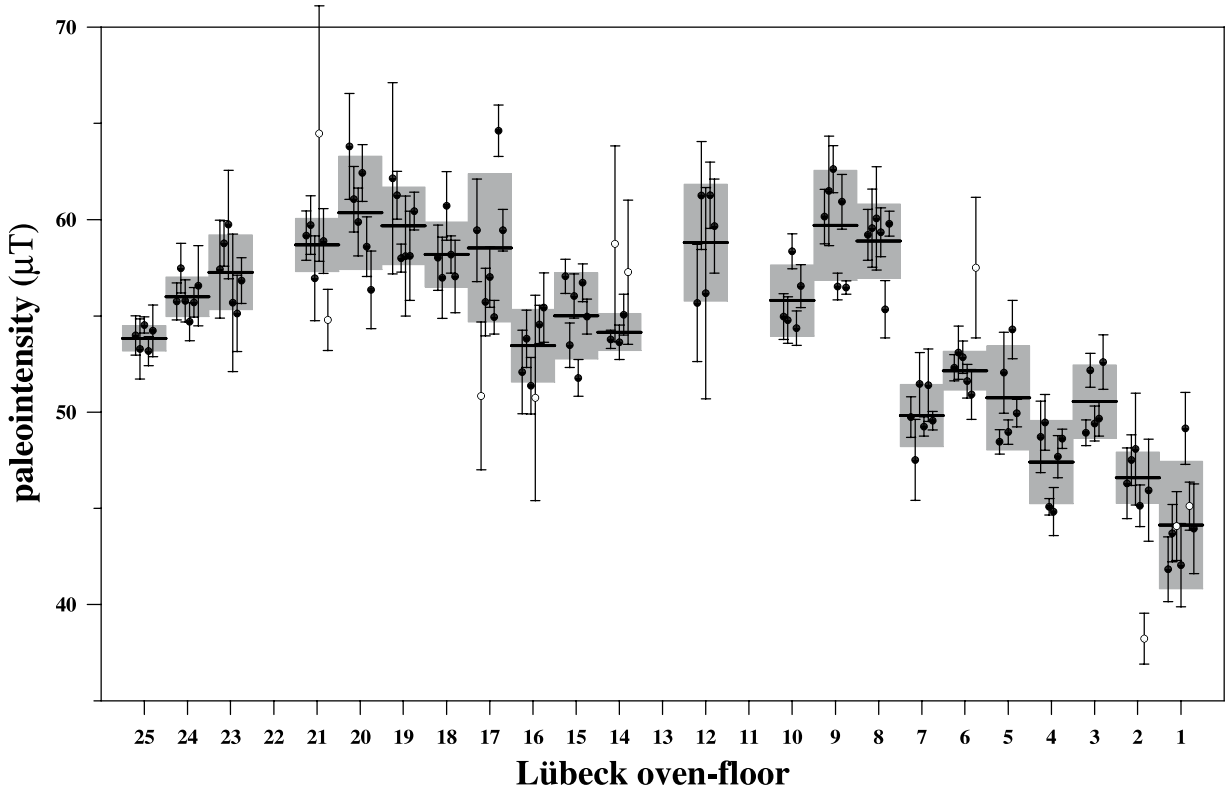

Figure 7. Individual Lübeck paleointensity results with standard error (dots, circles for rejected results) and unweighted mean with standard error (horizontal lines with gray bar) plotted versus number of oven floor layer.

in the curve calibration process, an average curve as well as a functional confidence envelop on the estimated curves is obtained. Details of the models and the applied algorithms have been reported by *Lanos* [2004] where univariate, bivariate, and full vector curve estimation have been discussed. Figure 8 shows the mean values versus time together with the three Bayesian curves of declination, inclination and intensity obtained from univariate Bayesian modeling in comparison with full vector Bayesian treatment (for curve data, see Table S2 in the auxiliary material). Univariate curves compare very well with full vector curves. Small differences are only seen for the error envelopes but no systematic contraction or expansion is seen. The data are well represented by the smoothed curves and they show patterns which are interpreted as secular variation of the EMF.

5.4. Comparison With Other Data

[27] Because the Lübeck oven floors provide a record of SV from about 1300 to 1750 A.D. the obtained Bayesian curves can be compared with global models of the EMF. For comparison the global model obtained from historical measurements of the EMF [*Jackson et al.*, 2000] was chosen, because this is a rather detailed model and completely independent from the Lübeck data. This is not true for the models of *Korte and Constable* [2005] or of *Pavón-Carrasco et al.* [2009] obtained from archaeomagnetic data sets which include the Lübeck directions. The CALS7K.2 model has also the disadvantage that it has a temporal and spatial resolution too low for our purpose [*Korte and Constable*, 2005]. The curves obtained from the *gufm1* model are shown as green lines in the diagrams (Figure 8). The *gufm1* model declination curve lies within the error envelopes of the Lübeck SV curves. Accordingly the agreement between both models is very good over the time interval where enough data are available. For inclination and intensity the agreement is less good but still reasonable. Here it has to be taken into account that records of inclination started at the end of the 17th century A.D. and for intensity one century later at the end of the 18th century. Accordingly the *gufm1* model may not resolve the secular variation very well at places or times for which no or few data contribute. Apart from this also the Lübeck data are not very well dated from the late 16th century until 1750 A.D. The Bayesian error modeling takes the stratigraphy into account and produces a smooth curve, which

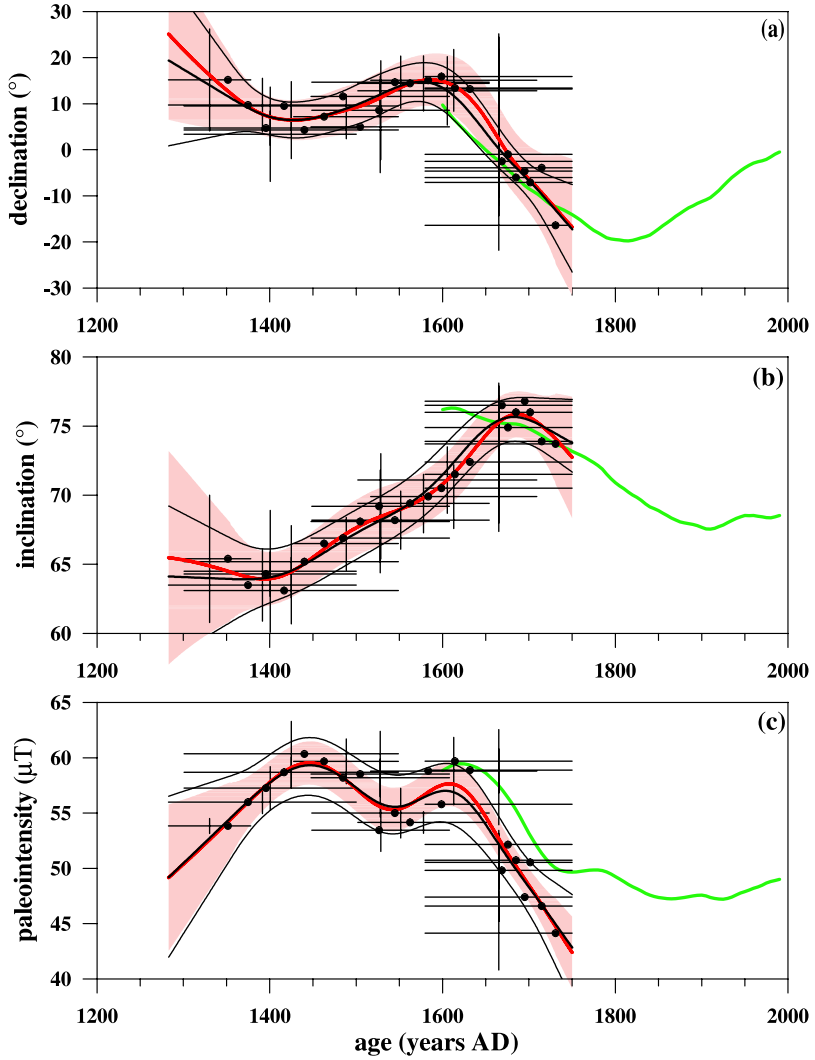

Figure 8. Full vector paleosecular variation obtained from the Lübeck oven floors. Error bars of (a) declination, (b) inclination, and (c) intensity are plotted versus time. Black dots on the time error bars indicate Bayesian posterior mean times. The bold red (black) lines are Bayesian curves obtained from full Bayesian vector treatment (univariate Bayesian modeling); the error bands are indicated by light red areas (thin black lines). The green lines are the magnetic elements calculated with the historical *gufm*1 model of *Jackson et al.* [2000] at Lübeck.

represents a best fit to the data. However, systematic errors in the dating might bias the curve, and so full vector data from more German sites would be needed to solve this problem.

[28] In order to compare the paleointensity curve obtained from Lübeck for the whole range of time, the paleointensity data compilation of *Chauvin et al.* [2000] has been supplied with more available data from western and central Europe covering the past 800 years. They were taken from 18 further studies [*Aitken et al.*, 1986; *Bucha*, 1967; *Burlatskaya et al.*, 1986; *Calvo et al.*, 2002; *Casas et al.*, 2005; *Catanzariti et al.*, 2008; *Czyszek and Czyszek*, 1987; *Gallet et al.*, 2005; *Genevey and Gallet*, 2002; *Gómez-Paccard et al.*, 2006, 2008; *Gram-Jensen et al.*, 2000; *Hill and Shaw*, 1999; *Kovacheva et al.*, 1995, 2004; *Kovacheva*, 1984; *Leonhardt et al.*, 2006; *Rolph*, 1997], most of them published after 2000. This data set is very similar to the one compiled recently by *Genevey et al.* [2008] although here are additional data while others are missing. Compared to the compilation of *Chauvin et al.* [2000] the large and very scattered data set from the United Kingdom is now balanced by also large data sets from Italy, Spain, Poland and Hungary (Figure 9a). The paleointensities (relocated to Lübeck) are strongly dispersed, but seem to form a band of about 20 μT in width showing a decrease

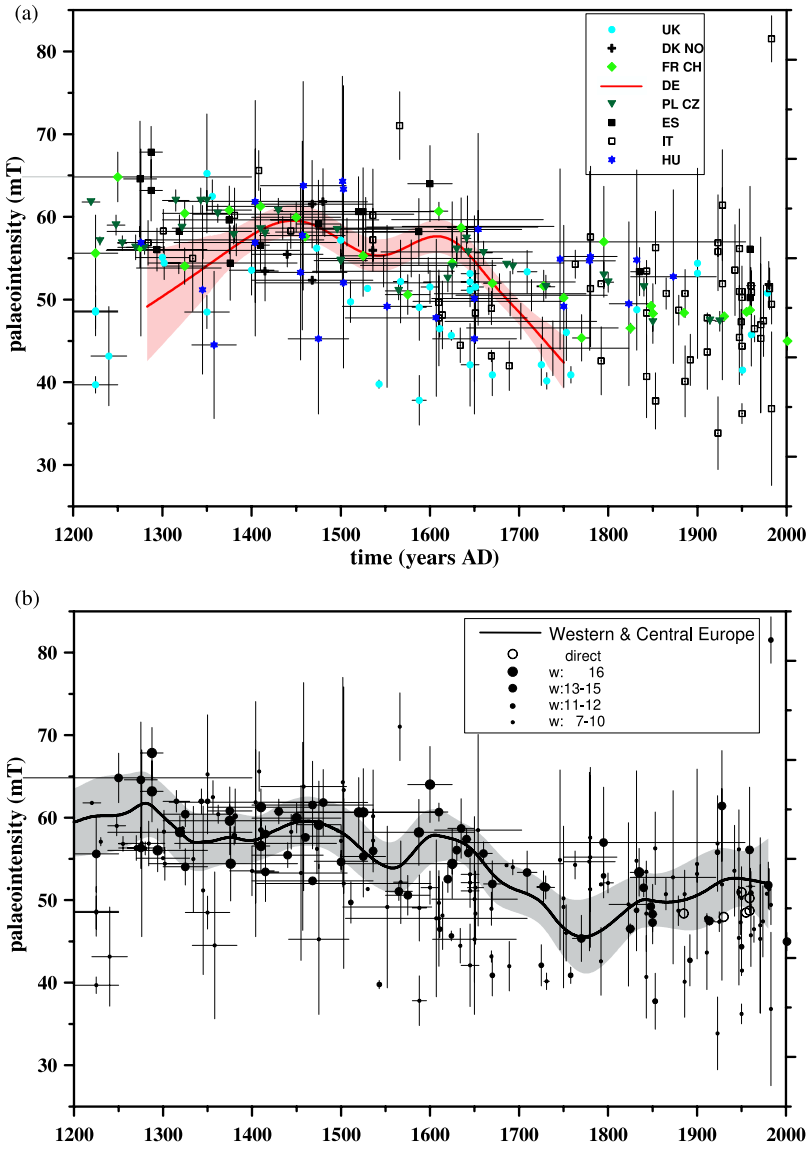

Figure 9. Paleointensity in western and central Europe during the time interval from 1200 to 2000 A.D., relocated to Lübeck (53.87°N, 10.81°E): (a) Data from volcanic rocks and archaeological material with 2σ error bars. Symbols indicate geographic location according to the legend. In red is shown the Lübeck curve from Figure 8 obtained from full Bayesian vector treatment. (b) Same data as in Figure 9a but quality (see text and Tables 2a–2c) is indicated by increasing size of the closed symbol according to the legend. Open symbols are direct observations. The bold black line is Bayesian curve with error envelope (gray area) obtained from univariate Bayesian modeling for selected data (see text).

from above 60 μT at 1200 A.D. to the present-day intensity of 49 μT at the reference site Lübeck (53.87°N latitude and 10.81°E longitude). Paleointensity in Lübeck decreased since the middle of the 17th century by about 25%, while another decrease can be seen around 1450 A.D. Maxima occur in the 15th and the early 17th century A.D. The Lübeck data are in good agreement with the archaeomagnetic paleointensity data from western and central Europe.

[29] The compiled paleointensity data have been classified using the same criteria as *Chauvin et al.* [2000] which means that three weights were defined relying on the reliability of the applied paleointensity technique (w_T), the kind of material (w_M) and the number of obtained individual paleointensity results (w_N) per site. The assigned weighting values are summarized in Tables 2a–2c. The Thellier or Coe's techniques with progressive heatings and pTRM checks were considered as the most reliable techniques when performed with

Table 2a. Weights Defined Relying on the Reliability of the Applied Paleointensity Technique[a]

w_T	Method	Cooling Rate Correction	Anisotropy Correction
6	Thellier or Coe	yes	yes
5	Thellier or Coe	no	yes
4	Thellier or Coe	no	no
4	Shaw	yes	yes
3	Shaw	no	yes
2	Shaw	no	no
1	other	-	-

[a] See text. w_T, applied paleointensity technique.

corrections of anisotropy of TRM and of cooling rate. In this case, w_T is maximal, or lower if no correction of cooling rate is performed. If the Thellier method, without any correction or the Shaw's method [*Shaw*, 1974], with corrections of anisotropy and cooling rate are used, $w_T = 4$. If corrections are missing w_T is lowered. For the other techniques (like *Rolph and Shaw* [1986] and *Tanguy* [1975]) w_T is only 1. Materials characterized usually by small anisotropy of TRM, like baked clay, bricks or lava flows were also preferred. In the cases of tiles w_T decreases, and further in the cases of pottery. When objects with a strong effect of shape are used, such as pipes, w_T has the lowest value. If the number of samples used per site is higher than five, w_N reaches the maximum of six, otherwise w_N is simply the number of samples used. The final weight associated with each average paleointensity is simply the addition of the three weights: $w = w_T + w_M + w_N$. The maximum weight possible is, therefore, 16, the minimum is three. Direct measurements from France [*Thellier and Thellier*, 1959] were given a weight of 20 [*Chauvin et al.*, 2000].

[30] Figure 9b shows the same data as Figure 9a but here the symbol size represents the obtained weight. Univariate Bayesian modeling was then applied to a selected data set which only includes paleointensity values from direct measurements or with weights of at least 13 (represented by the bigger dots). Only 74 values out of 250 paleointensities were left to do these calculations. The obtained curve with its error envelope (for curve data, see Table S3 in the auxiliary material) represents the selected data set well and it also shows a considerable variation, which seems very similar to the Lübeck curve shown in Figure 9a. Note, that these two paleointensity data sets are different, and so the curves are completely independent from each other. In order to demonstrate the agreement more clearly, the two curves are plotted together in Figure 10. The European curve compares very well to the Lübeck curve in the time interval from 1380 to 1700 A.D. and it is also in good agreement with the *gufm1* model. Beyond these times the Lübeck model curve is obviously distorted because of edge effects. Between 1200 and 1750 A.D. the paleointensity decreases from about 60 μT to 45 μT in western and central Europe. A similar decrease of 25% is observed by *Genevey et al.* [2008] for the virtual dipole moments from western Eurasia. But for this much larger region the decrease is almost linear, while for the data set presented here the western and central Europe curve shows local maxima at 1270 A.D., 1470 A.D., 1610 A.D. and 1930 A.D. and local minima at 1340 A.D., 1560 A.D. and 1770 A.D., and five of these extrema are supported by the Lübeck curve. Because both data sets are completely independent it seems that such a temporal variation can only be observed with the regional spatial and large temporal resolution used here but not yet with global compilations like the one of *Genevey et al.* [2008]. Surprisingly, the spherical cap harmonic model SCHA.DIF.3K of *Pavón-Carrasco et al.* [2009] does not show the same variation as the presented selected data set and the Lübeck oven floors do. The data set used by *Pavón-Carrasco et al.* [2009] does not use any data from Germany, but some from late medieval Danish sites, which are not far away from Lübeck. But most data come from eastern Europe and therefore intensity of this model may not be well constrained for central Europe. The SCHA.DIF.3K curve seems countercorrelated and instead of two maxima between 1400 and 1700 A.D.

Table 2b. Weights Defined Relying on the Kind of Material[a]

w_M	Material
4	baked clay, bricks or lava flows
3	tiles
2	pottery
1	small objects with a strong effect of shape: pipes

[a] See text. w_M, kind of material.

Table 2c. Weights Defined Relying on the Number of Obtained Individual Paleointensity Results per Structure[a]

w_N	Number of Paleointensity Determinations
6	6 or more
1–5	weight equal number of paleointensity determinations

[a] See text. w_N, number of obtained individual paleointensity results.

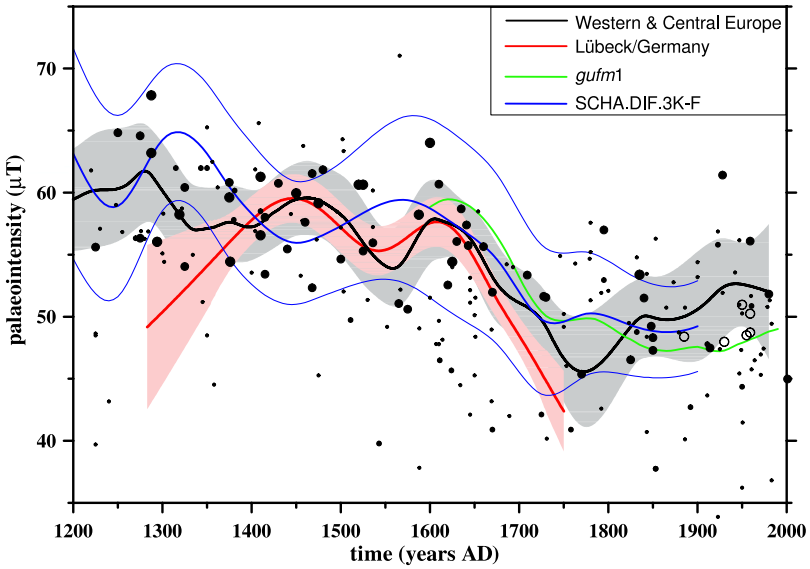

Figure 10. Comparison of paleointensity curves for data from western and central Europe during the time interval from 1200 to 2000 A.D., relocated to Lübeck (53.87°N, 10.81°E): the Lübeck curve from Figure 8 (full Bayesian vector treatment), the curve for western and central Europe from Figure 9b, *gufm*1 model as in Figure 8, and SCHA.DIF.3K model for the Lübeck site [*Pavón-Carrasco et al.*, 2009]. The paleointensity data are plotted also for comparison in the same way as in Figure 9b. Error bars are removed for clarity.

only one is seen (see Figure 10). This may be explained by the fact that the SCHA.DIF.3K model uses much more data from a larger region and that the database was not subjected to a selection process. However, the existence of two local intensity maxima in this time interval is also supported by new archaeomagnetic data from France and Italy [*Genevey et al.*, 2009]. As there is no good agreement with the new data from central and western Europe we like to emphasize that an intensity data selection is strongly recommended for modeling with spherical harmonics.

6. Conclusion

[31] A record of 450 years of full vector geomagnetic secular variation was obtained from a sequence of bread oven floors from Lübeck, Germany. The 22 reliable paleointensity estimates from this single site show a local minimum in the early 16th century and maxima in the early 15th century, another in the early 17th century. Then a decrease of about 20% until 1750 A.D. is observed, while inclination changes only a few degrees. This implies a strong decrease of the virtual dipole moment of the Earth's magnetic field since 1650 A.D.

[32] A compilation of the archaeomagnetic data set from western and central Europe shows very dispersed data which have a various quality. A selected data set was established relying on type of paleointensity method, kind of material and number of paleointensity determinations. The intensity curve obtained from Bayesian modeling of this data set compares very well with the one calculated from the Lübeck data. Both intensity curves show the same variations during the time interval 1300 to 1750 A.D. implying that intensity variations occur on time scales of centuries and less. Such small-scale variations are also seen in the global *gufm1* model derived from historical data. This model is in very good agreement with the Lübeck curve supporting the high quality obtained of paleomagnetic full vector data from these bread oven floors. On the contrary the spherical cap model SCHA.DIF.3K does not show a good agreement, neither with the intensity variation obtained from Lübeck nor with the curve calculated from the selected data set for western and central Europe. Therefore it seems that a selection of intensity data is absolutely necessary for intensity data, before using them for spherical harmonic models.

Acknowledgments

[33] Initial measurements have been carried out in the paleomagnetic laboratory of Montpellier with financial support from the Deutsche Forschungsgemeinschaft grant Schn 366/4-1 to 4. Thanks to M. Perrin for her cooperation. A 1 month stay of E.S. in Rennes was funded by a CNRS–University of Rennes

1 contribution (proper funding). Rock magnetic measurements were carried out in the paleomagnetic laboratory of the GFZ, Potsdam, during a stay of E.S. as guest scientist which was kindly supported by J.F.W. Negendank and N. Nowaczyk. R. Pucher and M. Müller contributed with helpful discussions on bread oven technique. The initial version benefited from helpful suggestions of the reviewers M. Korte and F. Donadini. The final work has been supported by the Austrian science fund grant P19370-N19.

References

Aitken, M. J., A. L. Allsop, G. D. Bussell, and M. B. Winter (1986), Paleointensity determination using the Thellier technique: Reliability criteria, *J. Geomagn. Geoelectr.*, *38*, 1353–1363.

Alexandrescu, M., V. Courtillot, and J.-L. Le Mouël (1997), High-resolution secular variation of the geomagnetic field in western Europe over the last 4 centuries: Comparison and integration of historical data from Paris and London, *J. Geophys. Res.*, *102*, 20,245–20,258, doi:10.1029/97JB01423.

Bucha, V. (1967), Intensity of the Earth's magnetic field during archeological times in Czechoslovakia, *Archaeometry*, *10*, 12–22, doi:10.1111/j.1475-4754.1967.tb00608.x.

Burlatskaya, S. P., P. Marton, and E. Marton (1986), The variation of the ancient geomagnetic field intensity for the territory of Hungary, *J. Geomagn. Geoelectr.*, *38*, 1369–1372.

Calvo, M., M. Prévot, M. Perrin, and J. Riisager (2002), Investigating the reasons for the failure of paleointensity experiments: A study on historical lava flows from Mt. Etna (Italy), *Geophys. J. Int.*, *149*, 44–63, doi:10.1046/j.1365-246X.2002.01619.x.

Carvallo, C., A. P. Roberts, R. Leonhardt, C. Laj, C. Kissel, M. Perrin, and P. Camps (2006), Increasing the efficiency of paleointensity analyses by selection of samples using first-order reversal curve diagrams, *J. Geophys. Res.*, *111*, B12103, doi:10.1029/2005JB004126.

Casas, L., J. Shaw, M. Gich, and J. A. Share (2005), High-quality microwave archaeointensity determinations from an early 18th century AD English brick kiln, *Geophys. J. Int.*, *161*, 653–661, doi:10.1111/j.1365-246X.2005.02631.x.

Catanzariti, G., G. McIntosh, M. Gómez-Paccard, V. C. Ruiz-Martínez, M. L. Osete, A. Chauvin, and T. A. S. Team (2008), Quality control of archaeomagnetic determination using a modern kiln with a complex NRM, *Phys. Chem. Earth, Parts A/B/C*, *33*, 427–437.

Chauvin, A., Y. Garcia, P. Lanos, and F. Laubenheimer (2000), Paleointensity of the geomagnetic field recorded on archaeomagnetic sites from France, *Phys. Earth Planet. Inter.*, *120*, 111–136, doi:10.1016/S0031-9201(00)00148-5.

Coe, R. S., S. C. Grommé, and E. A. Mankinen (1978), Geomagnetic paleointensities from radiocarbon-dated lava flows on Hawaii and the question of the Pacific nondipole low, *J. Geophys. Res.*, *83*, 1740–1756, doi:10.1029/JB083iB04p01740.

Czyszek, Z., and W. Czyszek (1987), Secular variations of the magnetic field in Poland from archaeomagnetic studies, *Acta Geophys. Polonia*, *35*, 187–215.

Day, R., M. Fuller, and V. A. Schmidt (1977), Hysteresis properties of titanomagnetites: Grain-size and compositional dependence, *Phys. Earth Planet. Inter.*, *13*, 260–267, doi:10.1016/0031-9201(77)90108-X.

Dunlop, D. (2002), Theory and application of the Day plot (M_{rs}/M_s versus H_{cr}/H_c): 2. Application to data for rocks, sediments, and soils, *J. Geophys. Res.*, *107*(B3), 2057, doi:10.1029/2001JB000487.

Gallet, Y., A. Genevey, and F. Fluteau (2005), Does Earth's magnetic field secular variation control centennial climate change?, *Earth Planet. Sci. Lett.*, *236*, 339–347, doi:10.1016/j.epsl.2005.04.045.

Genevey, A., and Y. Gallet (2002), Intensity of the geomagnetic field in western Europe over the past 2000 years: New data from ancient French pottery, *J. Geophys. Res.*, *107*(B11), 2285, doi:10.1029/2001JB000701.

Genevey, A., Y. Gallet, C. G. Constable, M. Korte, and G. Hulot (2008), ArcheoInt: An upgraded compilation of geomagnetic field intensity data for the past ten millennia and its application to the recovery of the past dipole moment, *Geochem. Geophys. Geosyst.*, *9*, Q04038, doi:10.1029/2007GC001881.

Genevey, A., Y. Gallet, F. Andreazzoli, C. Principe, M. L. Goff, G. Garzella, and M. Milanese (2009), Geomagnetic field intensity variations in western Europe during the past 800 years as inferred from architectural bricks sampled in Tuscany, Italy, *Geophys. Res. Abstr.*, *11*, EGU2009-4074.

Gómez-Paccard, M., A. Chauvin, P. Lanos, J. Thiriot, and P. Jiménez-Castillo (2006), Archeomagnetic study of seven contemporaneous kilns from Murcia (Spain), *Phys. Earth Planet. Inter.*, *157*, 16–32, doi:10.1016/j.pepi.2006.03.001.

Gómez-Paccard, M., A. Chauvin, P. Lanos, and J. Thiriot (2008), New archeointensity data from Spain and the geomagnetic dipole moment in western Europe over the past 2000 years, *J. Geophys. Res.*, *113*, B09103, doi:10.1029/2008JB005582.

Gram-Jensen, M., N. Abrahamsen, and A. Chauvin (2000), Archaeomagnetic intensity in Denmark, *Phys. Chem. Earth*, *25*, 525–531, doi:10.1016/S1464-1895(00)00081-8.

Hill, M. J., and J. Shaw (1999), Paleointensity results for historic lavas from Mt Etna using microwave demagnetization/remagnetization in a modified Thellier-type experiment, *Geophys. J. Int.*, *139*, 583–590, doi:10.1046/j.1365-246x.1999.00980.x.

Hill, M. J., P. Lanos, A. Chauvin, D. Vitali, and F. Laubenheimer (2007), An archaeomagnetic investigation of a Roman amphorae workshop in Albinia (Italy), *Geophys. J. Int.*, *169*, 471–482, doi:10.1111/j.1365-246X.2007.03362.x.

Jackson, A., A. R. T. Jonkers, and M. R. Walker (2000), Four centuries of geomagnetic secular variation from historical records, *Philos. Trans. R. Soc. London, Ser. A*, *358*, 957–990, doi:10.1098/rsta.2000.0569.

Jonkers, A. R. T., A. Jackson, and A. Murray (2003), Four centuries of geomagnetic data from historical records, *Rev. Geophys.*, *41*(2), 1006, doi:10.1029/2002RG000115.

Korhonen, K., F. Donadini, P. Riisager, and L. J. Pesonen (2008), GEOMAGIA50: An archeointensity database with PHP and MySQL, *Geochem. Geophys. Geosyst.*, *9*, Q04029, doi:10.1029/2007GC001893.

Korte, M., and C. Constable (2003), Continuous global geomagnetic field models for the past 3000, *Phys. Earth Planet. Inter.*, *140*, 73–89, doi:10.1016/j.pepi.2003.07.013.

Korte, M., and C. Constable (2005), Continuous geomagnetic field models for the past 7 millennia: 2. CALS7K, *Geochem. Geophys. Geosyst.*, *6*, Q02H16, doi:10.1029/2004GC000801.

Korte, M., A. Genevey, C. Constable, U. Frank, and E. Schnepp (2005), Continuous geomagnetic field models for the past 7 millennia: 1. A new global data compilation, *Geochem. Geophys. Geosyst.*, *6*, Q02H15, doi:10.1029/2004GC000800.

Kovacheva, M. A. (1984), Some archeomagnetic conclusions from three archaeological localities in north-west Africa, *C. R. Acad. Bulg. Sci.*, *37*, 171–174.

Kovacheva, M., J. Pares, N. Jordanova, and V. Karloukovski (1995), A new contribution to the archaeomagnetic study of a Roman pottery kiln from Calahorra (Spain), *Geophys. J. Int.*, *123*, 931–936, doi:10.1111/j.1365-246X.1995.tb06899.x.

Kovacheva, M., I. Hedley, N. Jordanova, M. Kostadinova, and V. Gigov (2004), Archaeomagnetic dating of archaeological sites from Switzerland and Bulgaria, *J. Archaeol. Sci.*, *31*, 1463–1479, doi:10.1016/j.jas.2004.03.019.

Kovacheva, M., A. Chauvin, N. Jordanova, P. Lanos, and V. Karloukovski (2009), Archaeointensity study of different archaeological structures. Anisotropy effect on the paleointensity results, *Earth Planets Space*, in press.

Lanos, P. (2004), Bayesian inference of calibration curves: Application to archaeomagnetism, in *Tools for Constructing Chronologies, Crossing Disciplinary Boundaries*, edited by C. E. Buck and A. R. Millard, pp. 43–82, Springer, London.

Lanos, P., M. Le Goff, M. Kovacheva, and E. Schnepp (2005), Hierarchical modelling of archaeomagnetic data and curve estimation by moving average technique, *Geophys. J. Int.*, *160*, 440–476, doi:10.1111/j.1365-246X.2005.02490.x.

Leonhardt, R., J. Matzka, A. R. L. Nichols, and D. B. Dingwell (2006), Cooling rate correction of paleointensity determination for volcanic glasses by relaxation geospeedometry, *Earth Planet. Sci. Lett.*, *243*, 282–292, doi:10.1016/j.epsl.2005.12.038.

Müller, U. (1992), Eine gewerbliche Bäckerie in Lübeck vom 13. bis zum 20. Jahrhundert. Ergebnisse der Grabung Mühlenstr. 65, in *Lübecker Schriften zu Archäologie und Kulturgeschichte*, vol. 22, pp. 123–143, Marie Leidorf, Rahden, Germany.

Pavón-Carrasco, F. J., M. L. Osete, J. M. Torta, and L. R. Gaya-Pique (2009), A regional archeomagnetic model for Europe for the last 3000 years, SCHA.DIF.3K: Applications to archeomagnetic dating, *Geochem. Geophys. Geosyst.*, *10*, Q03013, doi:10.1029/2008GC002244.

Rolph, T. C. (1997), An investigation of the magnetic variation within two recent lava flows, *Geophys. J. Int.*, *130*, 125–136, doi:10.1111/j.1365-246X.1997.tb00992.x.

Rolph, T. C., and J. Shaw (1986), Variations of the geomagnetic field in Sicily, *J. Geomagn. Geoelectr.*, *38*, 1269–1278.

Schlinger, C. M., D. R. Veblen, and J. G. Rosenbaum (1991), Magnetism and magnetic mineralogy of ash flow tuffs from Yucca Mountain, Nevada, *J. Geophys. Res.*, *96*, 6035–6052, doi:10.1029/90JB02653.

Schnepp, E. (2003), On correction of loss of mass during Thellier experiments, *Phys. Earth Planet. Inter.*, *135*, 225–229.

Schnepp, E., and R. Pucher (1998), Preliminary archaeomagnetic results from a floor sequence of a bread kiln in Lübeck (Germany), *Stud. Geophys. Geod.*, *42*, 1–11, doi:10.1023/A:1023348920652.

Schnepp, E., R. Pucher, C. Goedicke, A. Manzano, U. Müller, and P. Lanos (2003), Paleomagnetic directions and TL dating from a bread oven-floor sequence in Lübeck (Germany): A record of 450 years of geomagnetic secular variation, *J. Geophys. Res.*, *108*(B2), 2078, doi:10.1029/2002JB001975.

Shaw, J. (1974), A new method of determining the magnitude of the paleomagnetic field. Application of five historic lavas and five archeological samples, *Geophys. J. R. Astron. Soc.*, *39*, 133–144.

Tanguy, J. C. (1975), Intensity of the geomagnetic field from recent Italian lavas using a new paleointensity method, *Earth Planet. Sci. Lett.*, *27*, 314–320, doi:10.1016/0012-821X(75)90043-6.

Thellier, E., and O. Thellier (1944), Recherches géomagnetiques sur des coulées volcaniques d'Auvergne, *Ann. Geophys.*, *1*, 37–52.

Thellier, E., and O. Thellier (1959), Sur l'intensité du champ magnétique terrestre dans le passé historique et géologique, *Ann. Geophys.*, *15*, 285–376.

Yu, Y., and D. J. Dunlop (2003), On partial thermoremanent magnetization tail checks in Thellier paleointensity determination, *J. Geophys. Res.*, *108*(B2), 2523, doi:10.1029/2003JB002420.